Wettability-defined droplet imbibition in ceramic mesopores

Adnan Khalil[a], Felix Schäfer[a], Niels Postulka[a], Mathias Stanzel[a], Markus Biesalski[a], Annette Andrieu-Brunsen[a*]

Received 00th January 20xx,
Accepted 00th January 20xx

DOI: 10.1039/x0xx00000x

Wettability-defined liquid infiltration into porous materials in nature and several industrial applications is of fundamental interest. Direct observation of wetting-controlled imbibition in mesopores is anticipated to deliver important insights into the interplay between nanoconfined liquid movement and nanoscale wettability. We present a systematic study of water imbibition into mesoporous silica thin films with wetting properties precisely adjusted through chemical functionalization. We observe the liquid infiltration, resulting in an imbibition ring around the water droplet, by top-view imaging using a camera with collimated coaxial illumination. With decreasing hydrophilicity, the maximum imbibition area around the droplet decreases, accompanied by a simultaneous change in the imbibition kinetics and imbibition mechanism. Initially, the imbibition kinetics follow a modified Lucas-Washburn law that considers a strong influence of evaporation. However, with increasing imbibition time after reaching constant imbibition ring dimensions, the imbibition area starts to increase again, causing a deviation from the applied model. This observation is ascribed to water-mediated surface activation at the imbibition front, leading to a slightly increased wettability, which is also confirmed by water adsorption measurements. Furthermore, recently described spontaneous condensation-evaporation imbalances that cause oscillations of the imbibition front could be verified and were studied with regard to changing wetting properties. By increasing the contact angle of the material and therefore the partial pressure needed for capillary condensation, the amplitude of the imbibition front oscillations decreases. These results provide insights into the wettability-defined complex movement of water in mesoporous structures, which has practical implications, e.g., for nano/microfluidic devices and water purification or harvesting.

A. Introduction

In our everyday life, we encounter many processes based on liquid imbibition into a porous material, ranging from raindrops penetrating building walls to inkjet printing on paper. These processes are thus of extraordinary importance in both nature and technical applications. In nature, water is omnipresent within soils or the atmosphere, and its behavior in porous media is fundamental for, e.g., vascular flow in plants(1) and cloud formation via water condensation on small atmospheric particles(2). In technology, liquid imbibition is important for many applications, including several printing processes, oil recovery, porous material-based separation and cooling of microelectronic devices, among others.(3, 4) For this reason, the dynamics of liquid imbibition have been examined for many years, starting from the early works of Lucas(5) and Washburn(6) to recent studies of nanoporous materials(7, 8). In nanopores, the penetration of a wetting liquid has been reported to follow the classical Lucas-Washburn equation, even at the smaller end of the mesoscale. This holds true if evaporation can be neglected.(8-11) Additionally, driven by capillary condensation, pores on the nanoscale can be filled with water even in contact with an aqueous vapor phase. Thereby, capillary condensation can trigger an imbibition-like wetting front, whose dynamics can be described by a modified Lucas-Washburn equation.(12) In this context, Ceratti *et al.* demonstrated for hydrophilic mesoporous films that the natural liquid infiltration into the nanoporous material is determined by a cooperative mechanism, which involves liquid transport by capillarity and vapor transport by evaporation at the wetting front followed by capillary condensation.(9) These capillary phenomena governing mass transport are strongly defined by the porous structure and by evaporation, respectively.(9, 13) More recently, the group of Berli provided insights into the imbibition dynamics of water in mesoporous films by describing oscillations of the imbibition front that follow spontaneous condensation-evaporation imbalances caused by the hysteretic adsorption behavior of water in mesoporous materials.(7, 14, 15) Nevertheless, none of these studies considered the influence of the wetting of the nanopores on the imbibition or condensation-evaporation oscillation at the wetting front, although the contact angle has a significant influence on the dynamics of liquid propagation.(11) Correlation of the wetting properties with the liquid transport in a nanoconfined space would be of high interest, since the area of wetting phenomena is where chemistry, physics and engineering coincide.(16) Recently, we described the influence of wettability on the ionic transport in mesopores. By gradually adjusting the wettability, two transport paths for ions have been identified. By linking the condensation behavior, nanopore wall charge and wettability, a

[a] *Ernst-Berl-Institut für Technische und Makromolekulare Chemie, Technische Universität Darmstadt, 64287 Darmstadt, Germany.*
*Corresponding Author
†Electronic Supplementary Information (ESI) available. See
DOI: 10.1039/x0xx00000x

wetting regime in which a condensed water film forms that allows ionic transport along the pore wall has been described.(17)

In this study, we use mesoporous silica thin films and video recording of water-filled mesopores to investigate the influence of wettability on droplet imbibition and thereby water movement as well as the dynamic water front behavior in mesopores. We prepared mesoporous silica thin films by using evaporation-induced self-assembly via a simple dip-coating process. Our mesoporous films were used as nanoporous models to answer a number of fundamental questions. Firstly, we were interested in understanding the influence of wettability on the imbibition area around a droplet, deposited on the mesoporous surface. The wettability of the obtained mesoporous silica thin films was gradually adjusted by vapor phase deposition and covalent grafting of nonpolar silanes to the intrinsically hydrophilic silica material, as previously reported.(17) Next we addressed the question of the influence of the wetting properties on the imbibition kinetics and compared it to results from literature that did not consider wettability effects.(9, 15) Finally, we evaluated oscillations in the imbibition front with regard to designed wetting properties. We expect these results to have a strong impact on, e.g., lab-on-chip devices depending on the microenvironment. Furthermore, the wettability-designed imbibition properties of the mesoporous films present a promising alternative to creating patterned surfaces by utilizing the droplets' own Marangoni flow caused by solvent evaporation.(18-21) Thereby, the evaporation is strongly defined by the wettability and capillarity of the mesoporous material.

B. Experimental Section

Materials

Pluronic® F127 was purchased from Sigma-Aldrich. Tetraethoxysilane (TEOS) was purchased from Alfa Aesar, and 1H,1H,2H,2H-perfluorooctyl dimethylchlorosilane (PFODMCS) was purchased from Fluorochem. Ethanol (absolute) was purchased from Merck Millipore. All chemicals were used as received unless otherwise noted.

Mesoporous thin film preparation

Mesoporous silica thin films were prepared by sol-gel chemistry using Pluronic® F127 as a template in the presence of TEOS as a precursor in the following molar ratios: 1 TEOS:0.025 F127:34.5 H_2O:40 ethanol:0.08 HCl. The solution was stirred for 20 min before dip-coating with a withdrawal speed of 2 mm/s to produce thin films. The thin films were deposited on glass or silicon wafer (Si-Mat) substrates at a relative humidity (RH) of ~50 % and a temperature of ~25°C. Freshly deposited films were kept under these climate conditions for at least 1 h before being thermally treated. The films underwent two consecutive stabilization steps by heating them to 60°C within 10 min and holding this temperature for 1 h and then increasing the temperature to 130°C within 10 min and again holding it for 1 h. Then, the temperature was increased to 350°C at a rate of 1°C/min and held for 2 h for organic template calcination. Finally, the samples were rinsed with ethanol, leading to films with thicknesses of ~ 500-600 nm and a porosity of ~ 65 % as measured by ellipsometry and scanning electron microscopy (SEM).(23)

Vapor phase deposition of 1H,1H,2H,2H-perfluorooctyl dimethylchlorosilane

Vapor phase deposition of 1H,1H,2H,2H-perfluorooctyl dimethylchlorosilane (PFODMCS) was performed as described recently.(17) Briefly, the samples were cleaned with ethanol and dried with pressurized nitrogen before being placed in the reaction chamber (V = 1 L, room temperature). The chamber containing the samples was alternatingly evacuated and flushed with gaseous nitrogen three times before 10 µL of PFODMCS was placed into the chamber while applying a counterflow of nitrogen. Afterwards, a reduced pressure of 100 mbar was applied to the chamber and maintained for different time intervals. Finally, the samples were rinsed and extracted with toluene and ethanol before being stored under ambient conditions.

Ellipsometry

Ellipsometry was applied for reflecting silicon wafers (Si-Mat) using a Nanofilm Model EP3 imaging ellipsometer to determine the film thicknesses and refractive indices of the mesoporous thin films before and after functionalization. One zone angle of incidence (AOI) variation measurements were captured between 38° and 68° in steps of 2° with a 658 nm laser. The apparent film thicknesses and refractive indices were calculated from the measured ellipsometric angles Ψ and Δ using the EP4 analysis software supplied with the instrument. The measured data were fitted with a one-layer box model. The fitting range covered a film thickness from 400 to 700 nm and a refractive index range of 1 to 1.5. All films were measured at three identically marked positions before and after functionalization. The changes for each specific position were calculated, followed by mean value and error determination. To determine the porosity from the refractive indices, the Bruggemann effective medium approximation was used as described elsewhere.(24) Standard ellipsometry measurements were performed in air at a relative humidity (RH) of 20 %. To observe the sorption behavior of water in the mesoporous films, the RH-dependent refractive index change was monitored using humidity control (SolGelWay) according to Boissiere et al.(23) Prior to the actual sorption measurements the films were wetted and dewetted by exposing the samples to a gradual in-/ and decrease of RH in several steps:

1: Wetting: RH ~30% → RH ~45% → RH ~75% → RH ≥ 90%
2: Dewetting: RH ≥ 90% → RH ~75% → RH ~45% → RH ~ 30%
3: Sorption measurement depicted in Figure S5.

Contact angle

Contact angles (CAs) were measured as deposited with an OCA 35 device by DataPhysics Instruments using SCA 4.5.2 software and the sessile drop method under standard atmosphere (T = 23°C, RH = 50 %). A droplet volume of 2 µL was used, and the CA value was obtained by fitting the droplet shape using the approximation algorithm of the SCA software. The dynamic CA was measured by recording a video of an evaporating droplet followed by analysis of the receding CA by SCA 4.5.2 software.

Imbibition

The liquid imbibition from a water droplet into the mesoporous silica thin films was recorded with the Topview Video System TVS-C by Dataphysics. By using collimated coaxial illumination, the imbibition of water into the mesoporous films could be clearly recorded due to the high reflection from the imbibition area (depending on the supporting material; in this case, glass led to the best contrast between dry and wetted mesopores). The first 45 s were recorded with 37 frames per second (fps); afterwards, the amount of fps was reduced to 10 fps or 1 fps. The recorded videos were then evaluated with the help of the ImageJ image processing program and MATLAB. The spreading of the droplet as well as the progression of the imbibition front were measured in six different directions from the droplet center. By subtracting the width of the droplet from that of the imbibition front, the length of the imbibition ring around the droplet was calculated. The imbibition data shown in this manuscript are the arithmetic average over all six directions, unless otherwise noted. Exemplary videos (**Video S1-S4**) as well as the experimental setup (**Figure 1S**) can be found in the electronic supporting information of the article.

X-ray photoelectron spectroscopy (XPS)

XPS spectra were recorded using a Surface Science Laboratories SSX-100 X-ray photoelectron spectrometer equipped with a monochromatic Al Kα X-ray source (100 W). The X-ray spot size was 250-1000 µm. The binding energy scale of the system was calibrated using Au 4f7/2 = 84. eV and Cu 2p3/2 = 932.67 eV signals from foil samples. A Shirley background was subtracted from all spectra. Peak fitting was performed with Casa XPS using 70/30 Gaussian-Lorentzian product functions. Atomic ratios were determined from the integral intensities of the signals, which were corrected by empirically derived sensitivity factors.

C. Results & Discussion

Using sol-gel chemistry, evaporation-induced self-assembly(28) and dip-coating, mesoporous silica films were deposited on glass and silicon substrates. Tetraethyl orthosilicate (TEOS) served as a silica precursor, and the block copolymer Pluronic® F127 was utilized as a mesopore-forming template. In accordance with previous studies(26) and as determined by ellipsometry and electron microscopy, the applied mesoporous silica thin films had a thickness of ~ 500 - 600 nm (**Figure S2**), elliptical mesopores with pore diameters of 16 nm (**Figure 1 b**) and pore neck diameters of 12 nm, and a porosity of ~ 65 vol%.

To obtain a hybrid material and investigate the influence of wettability on water imbibition in mesopores, nonpolar 1H,1H,2H,2H-perfluorooctyl dimethylchlorosilane (PFODMCS) was postgrafted to the mesoporous silica material by vapor phase deposition, as recently described.(17) The time-dependent chemical surface functionalization allows gradual tuning of the functional group density, and as a consequence, the wetting properties can be gradually adjusted between ~20° and ~100°. To follow imbibition of water from a droplet on wetting adjusted mesoporous films, a top-view camera in combination with collimated coaxial illumination was applied. Time-dependent water droplet imbibition into an unmodified mesoporous film together with a schematic depiction is exemplified in **Figure 1**.

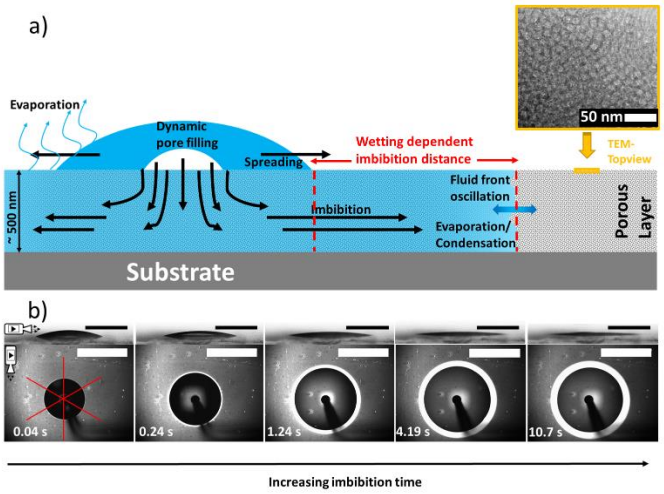

Figure 1. a) Schematic representation of water infiltration from a droplet into a mesoporous layer and the phenomena occurring simultaneously, as well as a TEM image of the mesoporous material. b) Side- (scale bar = 1 mm) and top-view imaging (scale bar = 2 mm) of droplet spreading and imbibition ring evolution. The red lines indicate the six different directions used to analyze the progression of the droplet and imbibition fronts.

Due to interconnections between the mesopores, the liquid is imbibed normal and lateral to the substrate surface, forming an imbibition ring around the water droplet deposited on top of the hydrophilic mesoporous silica film (**Figure 1 a**). This demonstrates that the liquid wets the pores not only directly underneath the droplet, but also ahead of the droplet three-phase contact line without being imbibed into the entire mesoporous film. Thereby, the liquid imbibition into mesoporous materials is governed by a cooperative mechanism consisting of liquid transport by capillarity and evaporation and condensation cycles at the liquid front (**Figure 1 a**), as already discussed by Ceratti et al.(9) Water is observed inside mesopores based on the local change in light reflectance, as water alters the refractive index compared to air-filled mesopores (see also **Video S1-S4**). In **Figure 1 b**, the propagation of the wetting front is pictured for a hydrophilic mesoporous silica thin film (as a reference; the corresponding contact angle measurements are shown in the SI, **Figure S3**). Due to direct coupling of the collimated coaxial light in the objective, the samples were illuminated parallel to the direction

of observation, causing a clear distinction between the droplet, air-filled pores and water-filled pores due to the high reflection of the light by water-filled mesopores. With increasing time, the droplet area as well as the length of the imbibition area (x(t)) increases until a maximum water droplet contact area as well as a maximum imbibition area is observed. This maximum droplet area as well as the maximum imbibition ring length is determined not only by the mesoporous structure, as discussed in the literature,(9) but also by the wettability-dependent imbibition and evaporation-condensation. Water evaporation from the droplet-air interface (**Figure 1 a**) creates a microclimate by forming a pressure (p) gradient, where the air adjacent to the water droplet is vapor saturated and the saturation level decreases to ambient conditions with increasing distance to the droplet.(7) According to the Kelvin equation, capillary condensation can occur in mesoporous layers in the vicinity of drops provided that the condensation pressure p_C is reached:

$$p_c = p_0 \exp\left(-\frac{2\gamma V_m \cos\theta}{r^* RT}\right) \quad (1)$$

(p_C = condensation pressure, p_0 = saturated vapor pressure, V_m = molar volume, r^* = Kelvin pore radius, γ = surface tension, R = gas constant, T = temperature, θ = contact angle)

At a certain distance from the droplet, when $p < p_C$, water no longer condenses in the mesopores.

To systematically understand the influence of wettability on imbibition, x(t) is analyzed in six different directions around the deposited water droplet, as indicated by the red lines in **Figure 1 b**. The clear differences in contrast were exploited using image analysis. In the process, we analyzed the time dependence of the water imbibition for a selection of samples with different deposited contact angles (CAs). The different wetting properties were established by vapor phase deposition of PFODMCS, schematically pictured in **Figure 2 a**.

The time-dependent imbibition resulting in an increasing length of the imbibition ring (x(t)) was evaluated until evaporation caused a receding of the water droplet three-phase contact line. In **Figure 2 b**, the effect of functionalization is most noticeable based on the fact that the maximum x(t) significantly decreases with increasing CA. While the reference sample (black, CA ~ 20°) exhibits an ~ 500 µm long imbibition ring, the ring gradually shrinks to ~ 300 µm (red, CA ~ 30°), then to ~ 200 µm (green, CA ~ 40°) and finally to ~ 100 µm (blue, CA ~ 50°) with increasing degree of functionalization. For CA ≥ 70°, no imbibition ring can be observed. Imbibition was still possible for CA ~ 60°, but the result is not shown here due to the low resolution during recording. The higher the CA is, the higher the partial pressure required to fill the mesopores by capillarity and condensation, which leads to decreasing x(t) with increasing CA until no imbibition can be observed.

To address the kinetics of the water imbibition, the squared imbibition length ($x(t)^2$) is considered (**Figure 3** and **Figure S4**),

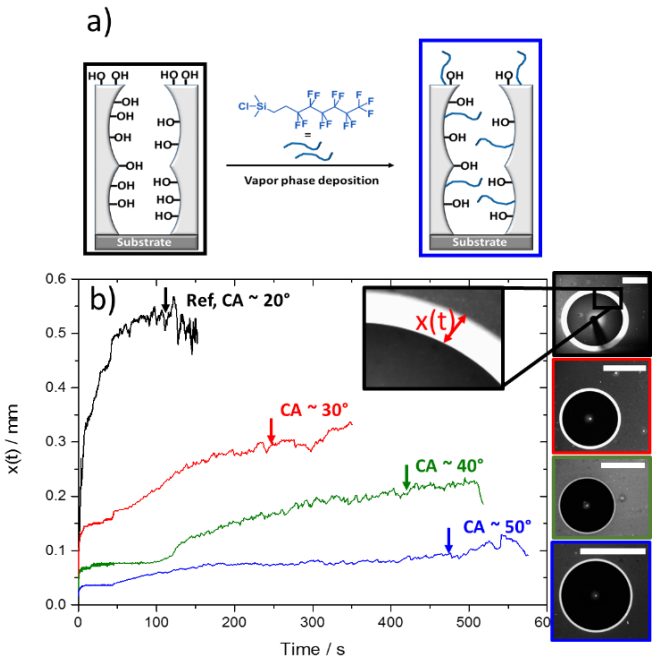

Figure 2. a) Functionalization of mesoporous silica films using vapor phase deposition of PFODMCS. b) Distance between the droplet front and the imbibition front (x(t)) as a function of the imbibition time (black: reference, CA ~ 20°; red: CA ~ 30°; green: CA ~ 40°; blue: CA ~ 50°; scale bar = 2 mm). The top-view images show the water droplet imbibition on mesoporous silica thin films with different degrees of functionalization leading to different CAs at the time marked by the colored arrows. The water imbibition is visible as an evolving white ring around the droplet (please note the scale bars; all scale bars = 1 mm).

since it is known from the literature that for mesopores, the Lucas-Washburn law is valid in the absence of evaporation. The Lucas-Washburn law describes a linear relationship between $x(t)^2$ and the imbibition time (t).(11, 27-29) However, water imbibition into thin films with film thicknesses << x(t) is strongly influenced by evaporation processes, which change the kinetics compared to conventional porous materials. Recently, Mercuri et al. elaborated a phenomenological model that combines the Lucas-Washburn law and surface evaporation to depict the filling dynamics of water in mesoporous thin films:(15)

$$x(t)^2 = x_{ss}^2\left[1 - \exp\left(-\frac{2t}{\tau}\right)\right] \quad (2)$$

(x(t) = length of the circular wetted region, x_{SS} = distance to the fluid front in the steady state, t = time, τ = evaporation time)

The first term dominates at short times, whereas the second term becomes more important at longer times, when the influence of evaporation becomes more dominant. The fluid front reaches a steady state position when both terms are equal. According to Mercuri *et al.*, the model appropriately described imbibition into mesoporous titanium films, whereas the imbibition behavior in mesoporous silica thin films was mentioned as being more complex due to the faster initial infiltration velocity and oscillations at the imbibition front.(15) With the setup applied in our work, we were able to temporally resolve the imbibition for short periods of time (t << 1 s, ~37 fps). Therefore, using the described equation as a fitting

function for the imbibition data shown in **Figure 2 b**, good agreement with the reference data (in terms of general shape, **Figure 3**) was observed. During the first short period of time, evaporation plays a subordinate role, and the imbibition shows a linear progression (in accordance with the Lucas-Washburn law). It takes approximately eight seconds until the influence of evaporation becomes noticeable, and the speed of imbibition decreases asymptotically. This aspect is well described by the fit used. The data also show that the imbibition front is not stationary but rather oscillating. Berli's group has described this effect as a consequence of the time-dependent imbalance between condensation and evaporation in hydrophilic silica mesoporous films.(7, 15) Before describing the fluid front oscillations in more detail, the influence of functionalization on the time-dependent imbibition will be discussed.

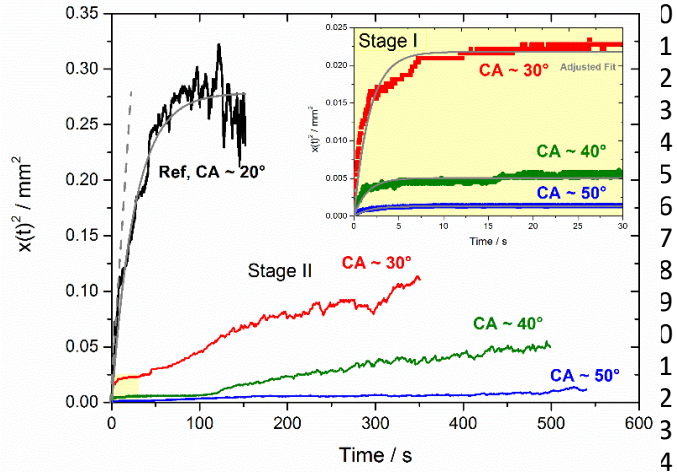

Figure 3. Squared imbibition length (x(t2)) of water in mesoporous silica thin films before and after functionalization (black: reference, CA ~ 20°; red: CA ~ 30°; green: CA ~ 40°; blue: CA ~ 50°). For all curves, the gray line corresponds to the fit using equation (1). The dotted gray line indicates the initial linear increase. The yellow-shaded area marks the first stage of imbibition after functionalization (Stage I), apparently following the modified Lucas-Washburn law. Afterwards, the imbibition front spreads again while oscillating (Stage II). For the reference sample, Stages I and II cannot be distinguished (also compare to SI, **Figure S3**).

As is evident from **Figure 3** and **Figure S3 b – d**, the functionalization and thus increased CA not only cause a decrease of the maximum $x(t)^2$ but also change its time-dependent evolution significantly and therefore cause a clear deviation from the abovementioned model for hydrophilic mesoporous films proposed by Mercuri *et al.*(15)

After functionalization, resulting in an increase of the CA, the imbibition seems to be divided into two different stages (**Figure 3**, Stages I and II). Before functionalization (black curve), when the samples are highly hydrophilic, the two stages cannot be distinguished, and the modified Lucas-Washburn law proposed by Mercuri *et al.*(15) describes the general progression of the imbibition front properly (while neglecting its oscillation). The imbibition data after silanization, when considering both stages, show a clear deviation from the applied model, especially with respect to Stage II (see **Figure S3**). However, the first stage (Stage I), up to approximately 30 s, is still in good agreement with the model of Mercuri *et al.* (**Figure 3**, yellow shaded region). In **Figure 3,** the zoom-in compares the first 30 s of water infiltration for different degrees of functionalization. For all CAs between 30° and 50°, a similar time-dependent evolution of $x(t)^2$ can be observed resembling the fit by the modified Lucas-Washburn equation (1). The initial imbibition ($t << 5$ s) is rapid (almost linear growth of x(t)). The slope of this initial increase decreases with increasing contact angle, as expected by the Lucas-Washburn law. After this initial increase, the time-dependent evolvement of the imbibition length then flattens until a plateau is reached. In this steady state of Stage I, no oscillations of the imbibition front can be detected. However, after varying periods of time, in a presumably stationary state, the imbibition front begins to advance again (**Figure 3** and **Figure S3**). This increase in $x(t)^2$ is much slower than that after initial contact of the surface and the droplet (Stage I). Furthermore, there is no real recognizable equilibrium. It seems that the imbibition ring continues to grow steadily with simultaneous oscillation of the fluid front until evaporation causes a receding of the droplet. When considering both stages, the deviation from the modified Lucas-Washburn model is caused by a renewed increase in the imbibition front (after long time periods ($t >> 30$ s)) x(t), with simultaneous oscillation until evaporation of the water droplet causes a receding of the three-phase contact line. This is addressed here as Stage II (**Figure 3** and **Figure S3 b – d**).

It is known from literature studies that the surface chemistry of silica materials can change through contact with water vapor or through water adsorption.(30-32) Water causes activation/increasing hydroxylation of the surface and thus a reduction in the hydrophobicity or an increase in the hydrophilicity. Taking into account this aspect and the mechanism by which water moves in a mesoporous silica thin film, namely, via multiple cycles of condensation and evaporation, we suspect that after a certain period of time, chemical changes of the surface at the imbibition front cause its renewed movement. When a functionalized mesoporous silica film (CA ~ 50°) was incubated in water, the CA decreased by ~8° (**Figure S6**), while the refractive index (measured by ellipsometry) remained constant (**Table S3**). This indicates surface activation rather than removal of the organic functional group. X-ray photoelectron spectroscopy (XPS) measurements support this hypothesis since the F/Si ratio of ~ 0.6 did not change after water incubation (**Figure S7** and **Table S4**), while the CA did.

The change in surface area due to water adsorption can also be seen in the water adsorption/desorption curves (**Figure S5**). All samples show a hysteresis after the adsorption and desorption of water that is not closed. This indicates that due to the change in surface area, water continues to adhere to the pores, which is also reported in the literature.(31)

The evaporation-condensation cycles that may cause slight changes in the mesopore walls can also be easily recorded with the optical setup used for imbibition length recording because, instead of reaching a state of equilibrium, the imbibition front

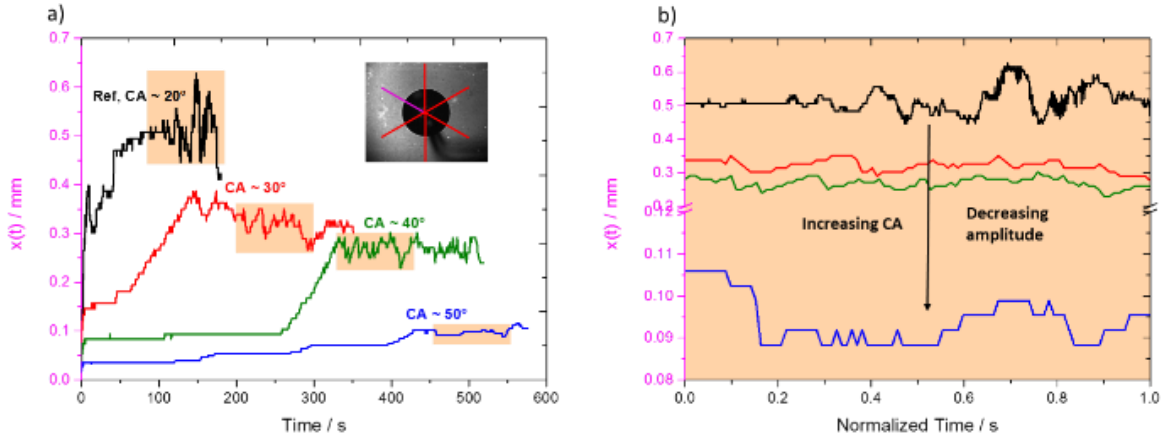

Figure 4. a) Comparison of x(t) for an unmodified reference sample and after different degrees of functionalization (black: CA ~ 20°, red: CA ~ 30°, green: CA ~ 40°, blue: CA ~ 50°). Only one direction of the imbibition front was considered (as indicated by the magenta line and axis). b) Comparison of the x(t) of the oscillating imbibition fronts in an interval of 90 s (normalized, indicated by the orange shade) after the initial, fast increase in the imbibition area (black: CA ~ 20°, red: CA ~ 30°, green: CA ~ 40°, blue: CA ~ 50°).

begins to oscillate. This is especially visible for the unmodified reference sample (**Video S1**). The functionalized samples show a different behavior. While the imbibition front is stable in Stage I and reaches steady values of ~ 0.022 mm², ~ 0.006 mm² and 0.001 mm² for CA ~ 30°, CA ~ 40° and CA ~ 50°, respectively, it spreads further under oscillation in Stage II. Thereby, x(t) reaches values of 0.11 mm² (CA ~ 30°), 0.06 mm² (CA ~ 40°) and 0.01 mm² (CA ~ 50°). The decrease in the CA due to surface activation induced by contact with water seems to have the effect that a range of partial pressures is reached over which the imbibition front oscillates noticeably, allowing imbibition to advance further.

In **Figure 4**, the oscillations at the imbibition fronts on the mesoporous silica thin films exhibiting different CAs are compared. The x-axis shows the normalized time for a period of 90 s in which the oscillations were most pronounced. For the functionalized samples, this occurs in Stage II (Ref.: 85 – 175 s, CA ~ 30°: 200 - 290 s, CA ~ 40°: 331 - 421 s, CA ~ 50°: 401 – 491 s).

For the unmodified reference sample (**Figure 4**), these oscillations are easily visible in the shown extracts as well as by eye in the recorded videos (**Video S1**), similar to the work by Mercuri *et al.* on unmodified mesoporous silica.(15) Before functionalization, the oscillation shows a maximum amplitude of ~ 150 µm, which rapidly decreases to ~ 50 µm after slight hydrophobization (CA ~ 30°). This is in accordance with the water sorption data in **Figure S5** and with the results that were recently published by our group.(17) The decrease in hydrophilicity upon chemical functionalization shifts the capillary condensation to higher relative humidities/critical vapor pressures for these porous systems. Even after minor surface modification (CA ~ 35°, red curve), the relative humidity at which capillary condensation occurs shifts by ~20 % to ~87 %. It must be noted that the apparent CA differs from the CA on the nanoscale. Under spatial confinement, the contact angle is higher(33) (see also **Figure S6**), which is why an apparently "slight" modification of the surface can have a strong effect on the sorption and imbibition of water since these phenomena are determined by small-scale events. As the partial pressure necessary for capillary condensation increases, the oscillations at the wetting front are reduced. This extends the observations made by Urteaga *et al.*(7) describing how the oscillations take the imprint of the hysteretic behavior of the mesoporous films. As shown in **Figure S5**, the hysteresis is determined not only by the porous structure(7, 9) but also significantly by the wettability. An increase in the CA causes a reduction in the amplitude of the water saturation, since the range of the pressure change in the hysteretic loop is decreased. Therefore, vapor pressure changes have a smaller effect on the position of the imbibition front.

For a higher CA of ~ 70°, the onset of capillary condensation shifts to RH > 90 %, and the condensation remains incomplete up to a partial pressure of 0.98. This is consistent with our observation that we could not record an oscillating imbibition front for contact angles ≥ 70°. By increasing the critical vapor pressure, the water can no longer penetrate or spread in the pores (**Figure 5 a**). In a previous study, we were able to define the degree of functionalization corresponding to a contact angle of 70° as the threshold value between water exclusion and imbibition.(17) At this value, the introduction of pore wall charge by increasing the solution pH to ten allowed water to condense without completely filling the pore volume. The effect f this phenomenon on possible radial spreading around the droplet and whether this can be followed visually was also investigated with the optical setup described above (**Figure 5 c**). At the threshold hydrophobicity, water cannot be imbibed and spread in the mesoporous film, due to the high critical infiltration pressure (**Figure 5 a** and **b**).

However, when adjusting the pH value of the water droplet to alkaline levels (pH = 10), the receding of the contact line at this threshold hydrophobicity, caused by evaporation, revealed the presence of water in the mesoporous silica thin film, but exclusively below the droplet (**Figure 5 c**). No imbibition ring (x(t) = 0) can be observed, because the water propagation at the threshold CA is fundamentally different from that at lower CA. The increased pH value generates surface charges in the silica material, which in turn induce film condensation of water in the mesopores.(17) In comparison, a water droplet with a pH value of two did not cause charge-induced condensation (**Figure 5 b**)

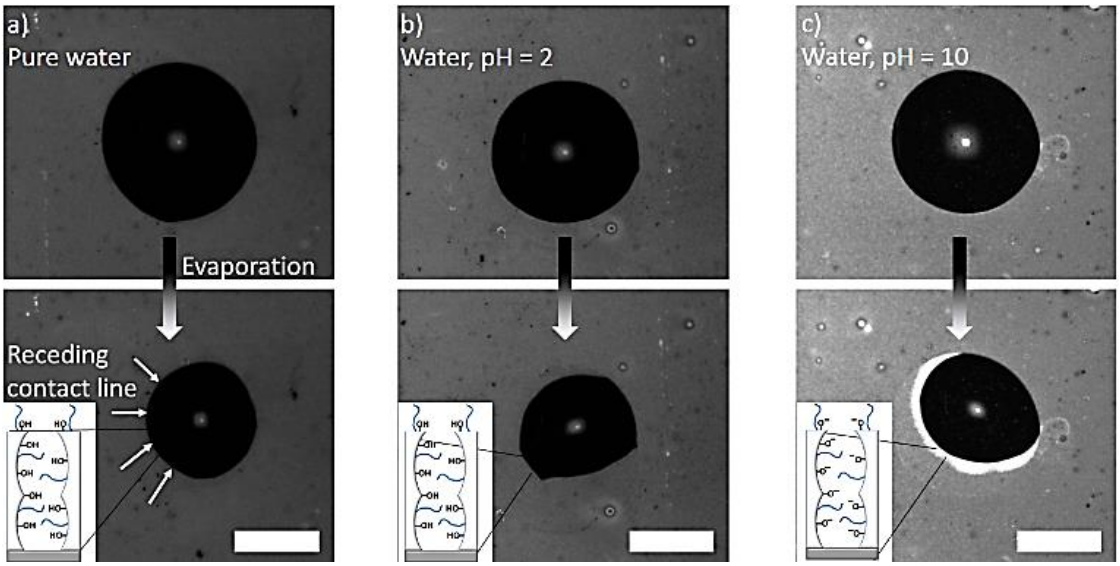

Figure 5. Top view of an evaporating droplet on mesoporous silica thin films exhibiting a CA of ~ 70°. a) Pure water, b) acidified water (pH = 2) and c) alkaline water (pH = 10) were used (scale bar = 1 mm).

Thus, we could show that the water droplet imbibition into mesoporous thin films can be controlled by the wetting properties. The mesoporous film wettability influences not only the kinetics of liquid propagation, but also its mechanism. Thereby, condensation plays a detrimental role with changing CA. Control of liquid propagation, as we could show here, for example, via wettability and/or charge, is highly interesting for many areas, especially in the field of nanofluidics for nanodevices.

Conclusions

In summary, the droplet imbibition of water into wettability adjusted mesoporous silica thin films is recorded with high temporal resolution to analyze the imbibition kinetics. The influence of wettability on fluid imbibition into mesoporous films is significant: not only does an increasing contact angle result in a reduced imbibition length, but also, it changes the kinetics by which this area is filled with water. Up to a contact angle of 60°, an imbibition range beyond the droplet three-phase contact line can be optically resolved. At a contact angle of 70°, imbibition occurs only if a negative charge is introduced into the system and exclusively below the droplet, i.e. no imbibition beyond the macroscopic contact line of the drop takes place. For even higher contact angles, liquid imbibition cannot be observed even directly below the drop. This is in accordance with a work previously published by our group.(17) When considering an unfunctionalized reference sample, imbibition is properly described by the modified Lucas-Washburn law presented by Mercuri *et al.*, which considers evaporation.(15) However, after hydrophobization, the model can only accurately describe the initial liquid propagation for short times. It is observed that the imbibition front advances again after some time. This is probably related to the activation of the silica surface by contact with water.(31, 32) The surface composition does not change during this process, as demonstrated by water adsorption combined with ellipsometry and contact angle measurements. Furthermore, an oscillating imbibition front, typical for mesoporous thin films, which was previously recorded only in Berli's working group(7, 15, 27), is confirmed. Through our experiments, the knowledge of these oscillations is extended with respect to wettability. As the contact angle increases, the amplitude of the oscillation decreases from ~ 150 µm (for an unmodified reference) to below 50 µm until the oscillation can hardly be detected. This effect can be explained by the increase in the partial pressure that must be achieved to allow condensation in the pores. This is verified by water adsorption curves.

The results obtained provide fundamental insights into the propagation mechanism of water in mesopores and its dependence on the wetting properties and are therefore of great importance for areas in which nanoporous materials are being increasingly in the focus of emerging applications, such as in sensor technology, catalysis and water treatment.

Conflicts of interest

There are no conflicts to declare.

Acknowledgements

We kindly acknowledge the financial support by the German Research Foundation (DFG) within the Collaborative Research Centre 1194 “Interaction between Transport and Wetting Processes”, Project <C04, A05>. In addition, the authors wish to thank Karl Kopp and Prof. Hess for X-ray Photoelectron Spectroscopy.

References

1. Stroock AD, Pagay VV, Zwieniecki MA, Michele Holbrook N. The physicochemical hydrodynamics of vascular plants. Annual Review of Fluid Mechanics. 2014;46:615-42.
2. Marcolli C. Deposition nucleation viewed as homogeneous or immersion freezing in pores and cavities. Atmospheric Chemistry and Physics. 2014;14(4):2071-104.
3. Zhang X, Liu H, Jiang L. Wettability and applications of nanochannels. Advanced Materials. 2019;31(5):1804508.
4. Gambaryan-Roisman T. Liquids on porous layers: wetting, imbibition and transport processes. Current Opinion in Colloid & Interface Science. 2014;19(4):320-35.
5. Lucas R. Ueber das Zeitgesetz des kapillaren Aufstiegs von Flüssigkeiten. Colloid & Polymer Science. 1918;23(1):15-22.
6. Washburn EW. The dynamics of capillary flow. Physical review. 1921;17(3):273.
7. Urteaga R, Mercuri M, Gimenez R, Bellino MG, Berli CL. Spontaneous water adsorption-desorption oscillations in mesoporous thin films. Journal of colloid and interface science. 2019;537:407-13.
8. Gruener S, Huber P. Capillarity-Driven Oil Flow in Nanopores: Darcy Scale Analysis of Lucas–Washburn Imbibition Dynamics. Transport in Porous Media. 2019;126(3):599-614.
9. Ceratti DR, Faustini M, Sinturel C, Vayer M, Dahirel V, Jardat M, et al. Critical effect of pore characteristics on capillary infiltration in mesoporous films. Nanoscale. 2015;7(12):5371-82.
10. Huber P. Soft matter in hard confinement: phase transition thermodynamics, structure, texture, diffusion and flow in nanoporous media. Journal of Physics: Condensed Matter. 2015;27(10):103102.
11. Gruener S, Huber P. Imbibition in mesoporous silica: rheological concepts and experiments on water and a liquid crystal. Journal of Physics: Condensed Matter. 2011;23(18):184109.
12. Vincent O, Marguet B, Stroock AD. Imbibition triggered by capillary condensation in nanopores. Langmuir. 2017;33(7):1655-61.
13. Liu M, Wu J, Gan Y, Hanaor DA, Chen C. Evaporation limited radial capillary penetration in porous media. Langmuir. 2016;32(38):9899-904.
14. Mercuri M, Berli CL, Bellino MG. Mesoporous thin films for fluid manipulation. Advanced Materials Interfaces. 2017;4(24):1700970.
15. Mercuri M, Pierpauli K, Bellino MG, Berli CL. Complex filling dynamics in mesoporous thin films. Langmuir. 2017;33(1):152-7.
16. Bonn D, Eggers J, Indekeu J, Meunier J, Rolley E. Wetting and spreading. Reviews of modern physics. 2009;81(2):739.
17. Khalil A, Zimmermann M, Bell AK, Kunz U, Hardt S, Kleebe H-J, et al. Insights into the interplay of wetting and transport in mesoporous silica films. Journal of colloid and interface science. 2020;560:369-78.
18. Parsa M, Harmand S, Sefiane K. Mechanisms of pattern formation from dried sessile drops. Advances in colloid and interface science. 2018;254:22-47.
19. Kabi P, Pal R, Basu S. Moses Effect: Splitting a sessile droplet using vapour mediated Marangoni effect leading to designer surface patterns. Langmuir. 2020.
20. Eom D, Chang J, Song Y-W, Lim J, Han J, Kim H, et al. Coffee-ring structure from dried graphene derivative solutions: a facile one-step fabrication route for all graphene-based transistors. The Journal of Physical Chemistry C. 2014;118(46):27081-90.
21. Brutin D, Sobac B, Loquet B, Sampol J. Pattern formation in drying drops of blood. Journal of fluid mechanics. 2011;667:85-95.
22. Bansal L, Sanyal A, Kabi P, Pathak B, Basu S. Engineering interfacial processes at mini-micro-nano scales using sessile droplet architecture. Langmuir. 2018;34(29):8423-42.
23. Boissiere C, Grosso D, Lepoutre S, Nicole L, Bruneau AB, Sanchez C. Porosity and mechanical properties of mesoporous thin films assessed by environmental ellipsometric porosimetry. Langmuir. 2005;21(26):12362-71.
24. Spanier JE, Herman IP. Use of hybrid phenomenological and statistical effective-medium theories of dielectric functions to model the infrared reflectance of porous SiC films. Physical Review B. 2000;61(15):10437.
25. Brinker CJ, Lu Y, Sellinger A, Fan H. Evaporation-induced self-assembly: nanostructures made easy. Advanced materials. 1999;11(7):579-85.
26. Herzog N, Brilmayer R, Stanzel M, Kalyta A, Spiehl D, Dörsam E, et al. Gravure printing for mesoporous film preparation. RSC advances. 2019;9(41):23570-8.
27. Acquaroli LN, Urteaga R, Berli CL, Koropecki RR. Capillary filling in nanostructured porous silicon. Langmuir. 2011;27(5):2067-72.
28. Dimitrov D, Milchev A, Binder K. Capillary rise in nanopores: molecular dynamics evidence for the Lucas-Washburn equation. Physical review letters. 2007;99(5):054501.
29. Xue Y, Markmann J, Duan H, Weissmüller J, Huber P. Switchable imbibition in nanoporous gold. Nature communications. 2014;5.
30. Matsumoto A, Sasaki T, Nishimiya N, Tsutsumi K. Evaluation of the hydrophobic properties of mesoporous FSM-16 by means of adsorption calorimetry. Langmuir. 2001;17(1):47-51.
31. Rathouský J, Thommes M. Adsorption properties and advanced textural characterization of novel micro/mesoporous zeolites. Studies in surface science and catalysis. 170: Elsevier; 2007. p. 1042-7.
32. Inagaki S, Fukushima Y. Adsorption of water vapor and hydrophobicity of ordered mesoporous silica, FSM-16. Microporous and mesoporous materials. 1998;21(4-6):667-72.
33. Boudot M, Ceratti DR, Faustini M, Boissière Cd, Grosso D. Alcohol-assisted water condensation and stabilization into hydrophobic mesoporosity. The Journal of Physical Chemistry C. 2014;118(41):23907-17.